Efford, M. G. & Boulanger, J. Fast evaluation of study designs for spatially explicit capture–recapture. Methods in Ecology and Evolution.

Appendix S1: Relationship between RSE for Poisson and binomial n

Given a value for $\mathrm{RSE}_P \equiv \sqrt{\mathrm{var}_P(\hat{D})}/\hat{D}$ and an arbitrary area A, what is the value of RSE_B? To answer this we draw on the literature for density estimates based on the conditional likelihood. Maximising the likelihood conditional on n provides estimates of the detection parameters (e.g., λ_0 and σ). These lead to the effective sampling area a (see below) and hence to Horvitz-Thompson-like estimates of density ($\hat{D} = n/\hat{a}$) (Borchers and Efford 2008). The estimates are identical to estimates from maximising the full likelihood (including D) when n is Poisson (Barker et al. 2014; Schofield and Barker 2016), and very similar when n is binomial.

Detection histories are observed only for those animals detected at least once during a study. The overall probability of detection for an individual centred at point $\mathbf{x}$ is an aggregate of its occasion- and detector-specific detection hazards $p_\cdot(\mathbf{x}) = 1 - \exp\{-\Lambda(\mathbf{x})\}$ (see main text). The effective sampling area $a = \int_{R^2} 1 - \exp\{-\Lambda(\mathbf{x})\}\, d\mathbf{x}$ is a useful scalar summary of the detection model when density is uniform.

A variance formulation for conditional likelihood estimates follows the partitioning used by Huggins (1989):

$$\mathrm{var}(\hat{D}) = s^2 + \hat{G}_\theta^T I^{-1} \hat{G}_\theta^T,$$

where I is the information matrix, $\hat{G}$ a gradient vector for $\hat{D}$ with respect to the detection parameters θ, and s^2 relates to variation in n. The term in I and $\hat{G}$ is common to both

models for n. Huggins considered the non-spatial binomial analogue, from which the spatial binomial case follows. For binomial n, $s_B^2 = (1 - a/A)na^{-2}$, where a is the effective sampling area and A is the nominal extent of the study area. For Poisson n we have $a/A \to 0$, and hence $s_P^2 = na^{-2}$. Some algebraic manipulation shows that the difference in RSE^2 depends only on $\mathrm{E}(N) = DA$:

$$\mathrm{RSE}_B = \sqrt{\mathrm{RSE}_P^2 - 1/(DA)}.$$

The relationship is exact for uniform density, when $\mathrm{E}(N) = \int D(\mathbf{x})\, d\mathbf{x} = DA$. We expect it to be an adequate approximation for most other studies.

Literature Cited

Barker, R. J., Schofield, M. R., Wright, J. A., Frantz, A. C., & Stevens, C. (2014). Closed-population capture–recapture modeling of samples drawn one at a time. Biometrics, 70, 775–782.

Borchers, D. L., & Efford, M. G. (2008). Spatially explicit maximum likelihood methods for capture–recapture studies. Biometrics, 64, 377–385.

Huggins, R. M. (1989). On the statistical analysis of capture experiments. Biometrika, 76, 133–140.

Schofield, M., & Barker, R. (2016). 50-year-old curiosities: ancillarity and inference in capture–recapture models. Statistical Science, 31, 161–174.

Efford, M. G. & Boulanger, J. Fast evaluation of study designs for spatially explicit capture–recapture. Methods in Ecology and Evolution.

Appendix S2: Expected number of movements

A movement or 'spatial recapture' (Royle et al. 2014) is a recapture (redetection) at a site other than the previous one. Movements are a subset of recaptures. We calculate the expected number of movements m by considering each recapture event in turn and calculating the conditional probability that it is at the same site as before. This is a sum of squared detector-wise conditional probabilities.

Conditional on detection somewhere, the probability of detection in detector k is $q_k(\mathbf{x}) = \lambda(d_k(\mathbf{x}))/\sum_k \lambda(d_k(\mathbf{x}))$. For clarity in the following detector-specific expressions we use $u(\mathbf{x}) = 1 - \exp\{-\Lambda(\mathbf{x})\})$ and $v(\mathbf{x}) = 1 - \sum_k q_k(\mathbf{x})^2$.

Count proximity detector ('count')

$$\mathrm{E}(m) = \int \{\Lambda(\mathbf{x}) - u(\mathbf{x})\} \times v(\mathbf{x}) \times D(\mathbf{x})\, d\mathbf{x}.$$

Multi-catch trap ('multi')

$$\mathrm{E}(m) = \int \{\sum_s p_s(\mathbf{x}) - u(\mathbf{x})\} \times v(\mathbf{x}) \times D(\mathbf{x})\, d\mathbf{x}.$$

Binary proximity detector ('proximity')

$$\mathrm{E}(m) = \int \{\sum_s \sum_k p_{ks}(\mathbf{x}) - u(\mathbf{x})\} \times v(\mathbf{x}) \times D(\mathbf{x})\, d\mathbf{x}.$$

Literature Cited

Royle, J. A., Chandler, R. B., Sollmann, R., & Gardner, B. (2014). Spatial capture–recapture. Waltham, MA: Academic Press.

Efford, M. G. & Boulanger, J. Fast evaluation of study designs for spatially explicit capture–recapture. Methods in Ecology and Evolution.

Appendix S3: Power calculation for comparison of two density estimates

We want to predict the power of a comparison between two independent surveys as a function of the effect size defined as the ratio of the final density to the initial density (D_2/D_1) and the predicted precision of the estimates, expressed as relative standard error RSE. The power calculation assumes log-normal errors in both the initial and final surveys. Log-normal errors are natural for estimates of density (we use a log link function for maximising the likelihood, and rely on symmetrical Wald intervals on the log scale).

For a log normal distribution the variance on the log scale is $\sigma^2 = \log(1 + \mathrm{CV}^2)$ where CV is the coefficient of variation on the arithmetic scale (equivalent here to RSE). The mean μ on the log scale is related to the mean m on the arithmetic scale by $\mu = \log \frac{m}{\sqrt{1+\mathrm{CV}^2}}$.

We conduct a z-test on the log scale. The effect size on the log scale is $\mu_2 - \mu_1$. In general we must allow for differing RSE in the two surveys, which affects both the effect size and its variance, as follows.

$$\mu_2 - \mu_1 = \log \frac{m_2}{\sqrt{1 + \mathrm{CV}_2^2}} - \log \frac{m_1}{\sqrt{1 + \mathrm{CV}_1^2}}.$$

This reduces to

$$\mu_2 - \mu_1 = \log \frac{m_2}{m_1} + \log \frac{\sqrt{1 + \mathrm{CV}_1^2}}{\sqrt{1 + \mathrm{CV}_2^2}}.$$

For equal CV the second term drops out.

The variance of the effect on the log scale is approximated by the sum of the

respective variances:

$$\sigma_{21}^2 = \log(1 + \mathrm{CV}_1^2) + \log(1 + \mathrm{CV}_2^2).$$

The standardised difference on the log scale $\frac{\mu_2 - \mu_1}{\sigma_{21}}$ is compared to a standard normal variate at the desired alpha level.

In our application we replace m_2/m_1 by D_2/D_1 and CV_1 by RSE. To adjust for density-dependent RSE we assume that the change in RSE between surveys is inversely proportional to the square root of D_2/D_1 (this follows the logic of the approximation rse_P in which both $\mathrm{E}(n)$ and $\mathrm{E}(r)$ scale with density). Thus $\mathrm{CV}_2 = \mathrm{RSE} \times \frac{1}{\sqrt{D_2/D_1}}$.

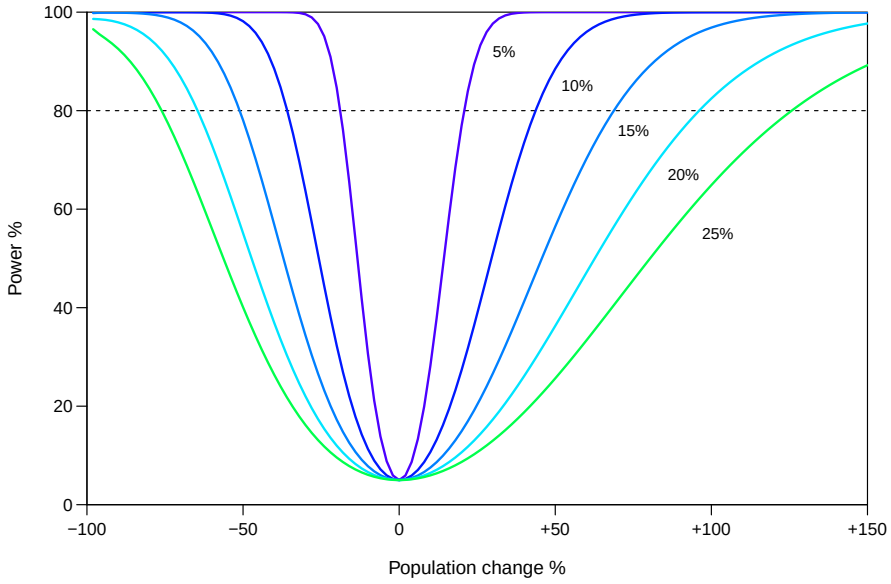

Fig. S1. Power of a 2-sided test ($\alpha = 0.05$) for change between two surveys given different levels of the initial $\mathrm{RSE}(\hat{D}_1)$; $\mathrm{RSE}(\hat{D}_2)$ for the final survey is scaled by $\sqrt{D_1/D_2}$

Appendix S4. Simulations to evaluate RSE approximation

Simulations reported in main text Fig. 2.

The precision of SECR density estimates was evaluated using binary proximity data simulated for square grids of three sizes (6×6, 8×8, and 10×10) with detector spacings $0.25\sigma, 0.5\sigma, ..., 3.25\sigma$ sampled on 5 occasions. Density was held constant at $0.4\sigma^{-2}$. Detection hazard followed a half-normal curve with intercept parameter $\lambda_0 = 0.2$ or $\lambda_0 \in \{0.05, 0.1, 0.2\}$ (constant grid size 10×10). Density was estimated by maximising the log likelihood with the function 'openCR.fit' in Efford (2019a); integrals were approximated by summation over a grid of 0.5σ pixels extending 4σ beyond the detectors. 200 replicate simulations were performed for each scenario. Results for grids are shown in the main text Fig. **??**. R code and output are provided in the supplementary material at Zenodo https://doi.org/10.5281/zenodo.3239532. .

Additional simulations

Further sets of simulations were conducted with variations on the preceding scenarios (constant intercept parameter $\lambda_0 = 0.2$).

1. Alternative detector types (multi-catch traps and Poisson count proximity detectors)

2. Lines of 10 or 40 detectors with density $2\sigma^{-2}$ (emulating 5 independent lines at $0.4\sigma^{-2}$).

3. Overdispersed activity centres generated from Neyman-Scott distribution with mean 10 centres per cluster and within-cluster spread parameter σ_h equal to halfnormal detection σ. Activity centres falling outside the arena were wrapped to the opposite edge. Sampling with 10×10 grid of binary proximity detectors over 5 occasions with $\lambda_0 = 0.2$, as in main simulations.

R code and output are provided in the supplementary material. Results for multi-catch traps and count proximity detectors are shown in Fig. S3. Results for lines are shown in Fig. S4.

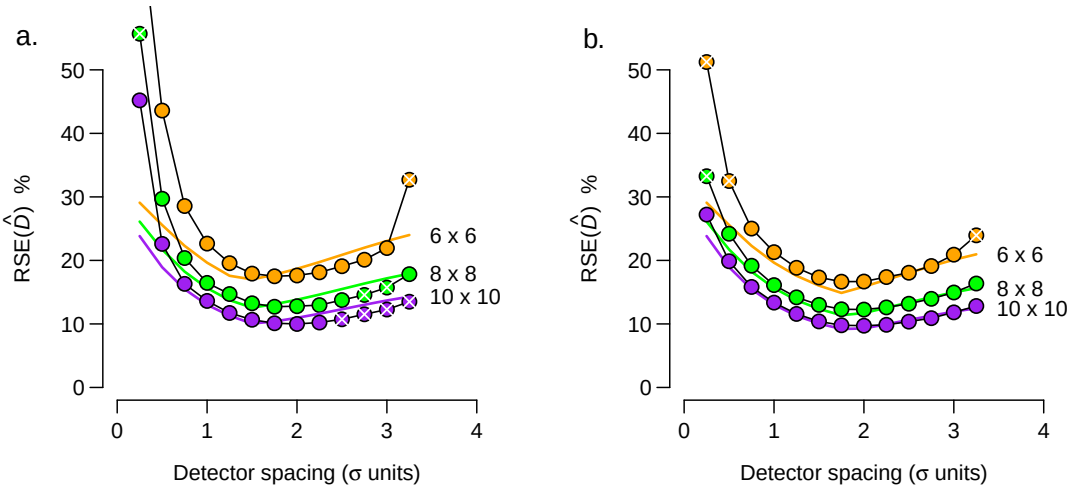

Fig. S3. Approximate and simulated RSE of density estimates as a function of detector spacing for square grids of (a) multi-catch traps and (b) count proximity detectors. The approximate RSE rse_P is shown as a solid line and simulated RSE as points. Simulated scenarios with relative bias of density estimate $> 5\%$ marked with white $\times$.

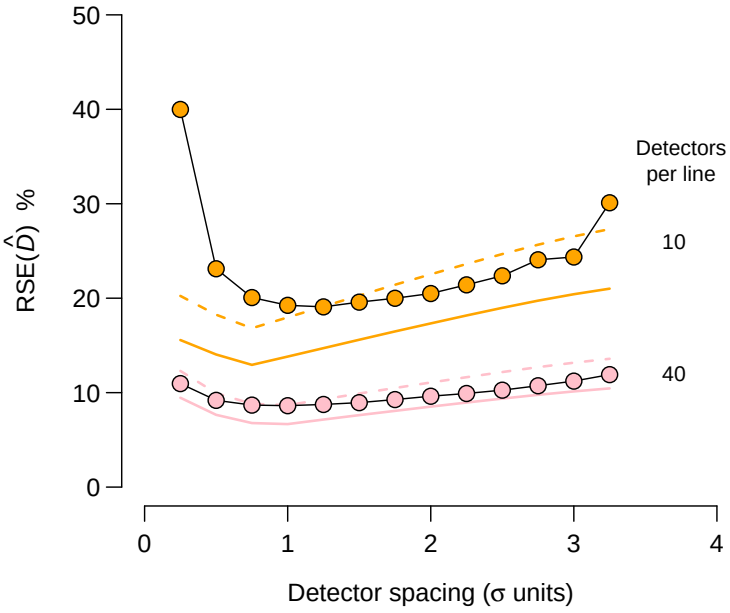

Fig. S4. Approximate and simulated RSE of density estimates as a function of detector spacing for linear arrays. The approximate RSE rse_P is shown as a solid line and simulated RSE as points. The dashed lines show the approximation increased by a factor of 1.3.

The single overdispersed scenario resulted in underestimation of the sampling variance and more than doubled the empirical RSE($\hat{D}$) relative to both the naive (uniform-model) $\widehat{\text{RSE}}(\hat{D})$ and the approximation (Fig. S5).

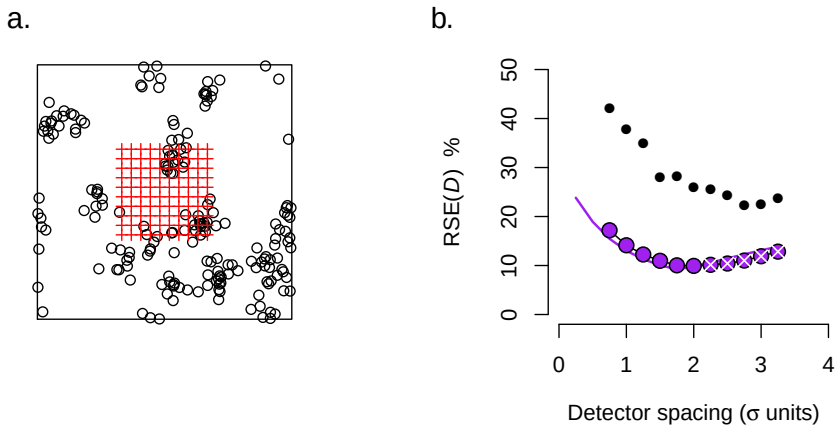

Fig. S5. Effect of strong overdispersion on the precision of density estimates from Poisson model. (a) Example of overdispersed activity centres generated from a wrapped Neyman-Scott distribution with $\mu = 10$ expected animals per cluster and within-cluster spread $\sigma_h = \sigma$; (b) Empirical estimate of $\widehat{\mathrm{RSE}}(\hat{D})$ based on the variance from 200 replicate simulations (isolated points) compared to $\mathrm{RSE}_P(\hat{D})$ estimated from naive Poisson model (connected points) and approximation (solid line). Simulations for spacings 0.25σ and 0.5σ omitted because some failed.

Timing

Timings were compared on a desktop machine with Intel Core i7 CPU (2.93 GHz). For many purposes an adequate prediction of $\mathrm{RSE}(\hat{D})$ may be obtained without maximising the likelihood merely by numerically evaluating the information matrix at know parameter values ('non-MLE'). Also, for predicting $\mathrm{RSE}(\hat{D})$ alone, 200 replicates is excessive, especially for the non-MLE method. For timing purposes we therefore conducted further simulations with the grids of proximity detectors using the same 5 scenarios for each of 13 detector spacings as in main text Fig. 2, but with only 20 replicates. This yielded median SE of the mean $\mathrm{RSE}(\hat{D})$ across replicates of about 0.1%.

Estimates of RSE($\hat{D}$) from the short-cut simulation procedure (non-MLE) are plotted against estimates from a larger number of full simulations in Fig. S6. There is no evidence for systematic bias, and the agreement is very good for RSE($\hat{D}$) $< 25\%$.

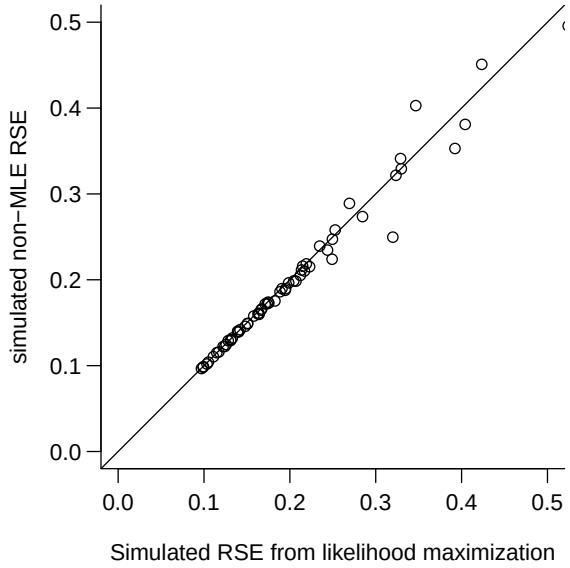

Fig. S6. Comparison of simulated non-MLE and MLE RSE of density estimates. 20 replicates for non-MLE and 200 replicates for MLE.

Table S1. Timings for two simulation-based methods for predicting RSE($\hat{D}$) (MLE, non-MLE; both 20 replicates) compared to an approximation using the expected sample size. Aggregate execution time for 5 scenarios at each of 13 detector spacings (cf Fig. 2 of the main text). The precision of the simulation-based methods is indicated by SE(RSE); this is the median across scenarios and detector spacings of the standard error of the mean RSE($\hat{D}$) (RSE expressed as percentage).

Method	SE(RSE)	Time (s)	Relative time
MLE	0.41	21928.2	1227.1
non-MLE	0.14	3839.7	214.9
Approximation	—	17.9	1.0

Literature Cited

Efford, M. G. (2019a). openCR: Open population capture–recapture models. R package version 1.3.3. https://CRAN.R-project.org/package=openCR [accessed 25 January 2019]

Efford, M. G. (2019b). secr: Spatially explicit capture–recapture models. R package version 3.2.0. http://CRAN.R-project.org/package=secr [accessed 25 January 2019]

Appendix S5: Comparison with published simulations

Extensive simulations to evaluate SECR sampling designs were recently undertaken by Kristensen and Kovach (2018) and Clark (2019). The simulation results archived by these authors are compared here to the fast approximation described in the main paper ($\mathrm{rse}_P(\hat{D}) = 1/\sqrt{\min\{\mathrm{E}(n), \mathrm{E}(r)\}}$).

Kristensen and Kovach (2018) estimated the density of New England cottontail rabbits (*Sylvilagus transitionalis*) using DNA from fecal pellets collected at intervals along transects after fresh snowfall. They used simulation to evaluate 105 sampling designs varying the number of sampling occasions (1, 2, 3), spacing along transects (20, 30, 40, 50, 60 m) and spacing between transects (30, 40, 50, 60, 70, 80, 90 m), at 4 different densities (0.5, 1, 2, 3 rabbits per hectare). Detection parameters were constant ($g_0 = 0.1$, $\sigma = 50$ m).

Clark (2019) considered designs using clusters of DNA hair snags for female American black bears (*Ursus americanus*). Most of his simulations assumed independence among clusters (no recaptures between clusters) and these are the results considered here. The simulations represent 203 different scenarios for combinations of density ($D = 0.05, 0.15, 0.30\mathrm{km}^{-2}$), detection parameters ($g_0 = 0.05, 0.1, 0.2$, $\sigma = 1, 2, 3\mathrm{km}$), cluster size ($2\times2, 3\times3, 4\times4, 5\times5$), number of sampling occasions (4, 6, 8), spacing of detectors within clusters (0.5, 1.0, 1.5, 2, 2.5, 3, 3.5, 4 km), spacing of clusters (10, 12, 14, 16, 18, 20, 25, 30 km) and total size of study area (2500, 10000, 20000, 40000 km^2) (Clark 2019, Tables S1–S9).

In both sets of simulations detectors were modelled as binary proximity detectors, a half-normal detection function was used, the variance calculation assumed Poisson rather than fixed N, and results for each scenario were sumarised as relative bias (RB) and relative standard error (RSE) averaged over 100 replicates.

We computed E(n) and E(r) for each scenario using the default spatial discretisation in secrdesign (Efford 2019) (square grid of $32 \times 32 = 1024$ points). The algorithm used a half-normal function for detection hazard, rather than for detection probability; parameters λ_0 and σ for each hazard function were adjusted to give a probability curve closely matching that specified by g_0 and σ (coded in the secrdesign function 'scenarioSummary').

Scenarios were identified as 'extreme' by criteria appropriate to each study. For Kristensen and Kovach (2018), the criterion was that likelihood maximisation failed in at least three replicates, usually due to very few spatial recaptures. For Clark (2019) the criterion was that the diagonal of a cluster was less than the diameter of a 95% activity contour (4.9σ; this assumes the hazard of detection is directly proportional to intensity of space use).

Execution of 'scenarioSummary' to compute E(n), E(r) and related variables took 35 seconds for the cottontail scenarios and 6 seconds for the black bear scenarios (Intel Core i7 CPU 2.93 GHz).

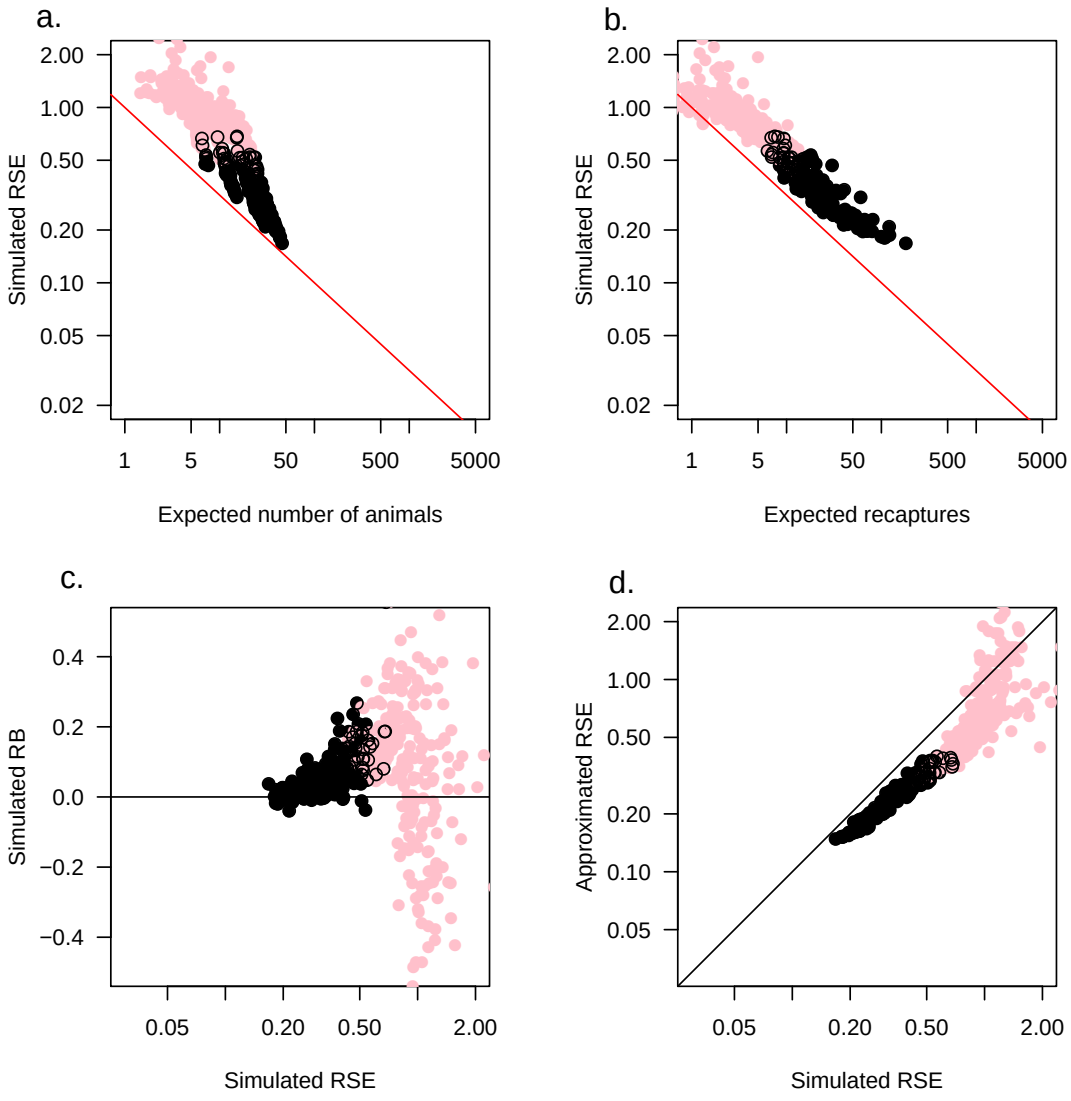

Fig. S7. Simulated RSE of density estimates for New England cottontails (Kristensen and Kovach 2018) summarised and related to expected counts for the same scenarios. Scenarios in pink were identified as extreme because estimation failed in at least 3 of 100 replicates. (a) RSE($\hat{D}$) vs E(n), (b) RSE($\hat{D}$) vs E(r), (c) RB($\hat{D}$) vs RSE($\hat{D}$), (d) $1/\sqrt{\min\{\mathrm{E}(n), \mathrm{E}(r)\}}$ vs RSE($\hat{D}$).

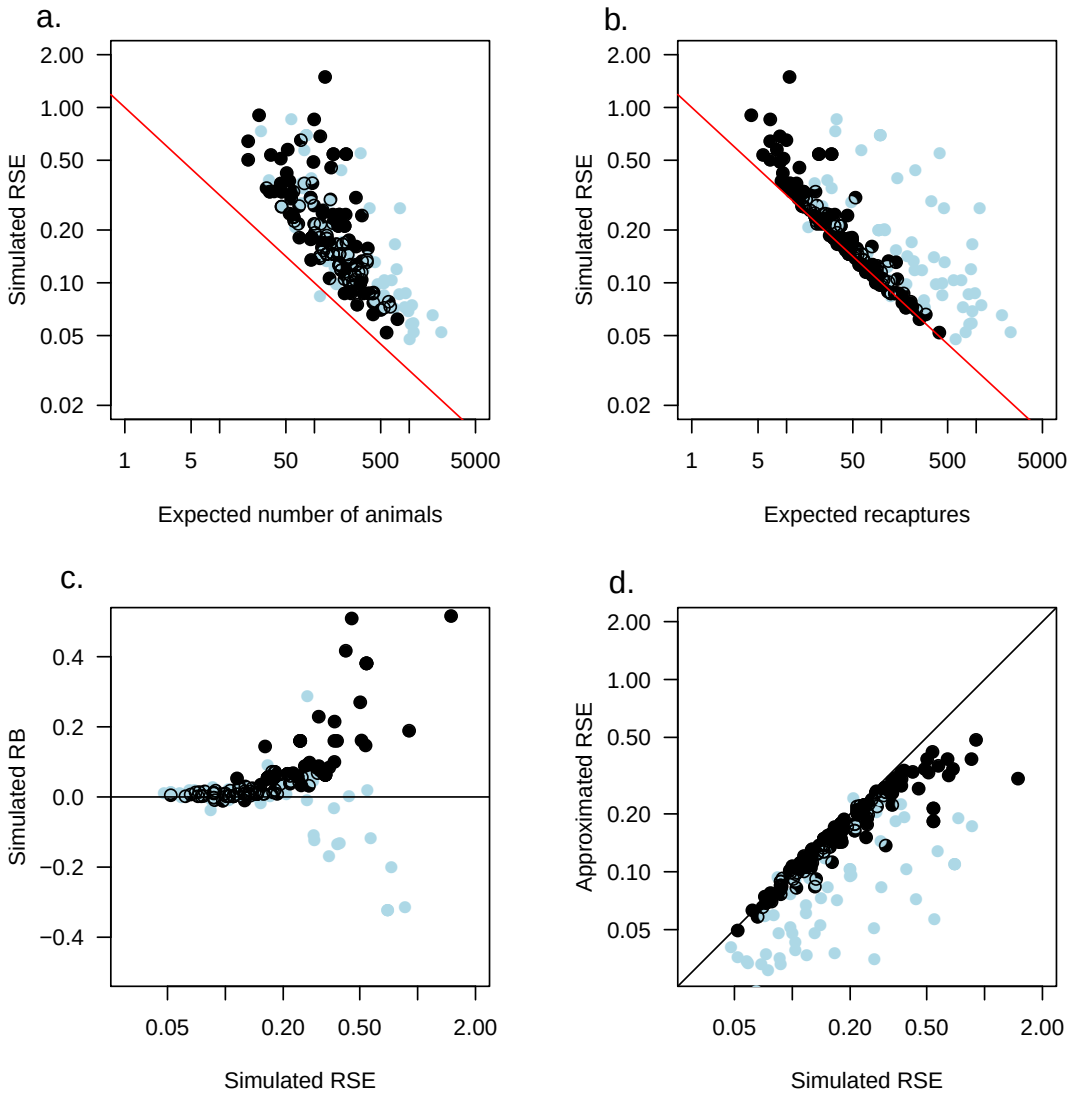

Fig. S8. Simulated RSE of density estimates for black bears (Clark 2019) summarised and related to expected counts for the same scenarios. Scenarios in pale blue were identified as extreme because the cluster diagonal was less than 4.9σ. (a) RSE($\hat{D}$) vs E(n), (b) RSE($\hat{D}$) vs E(r), (c) RB($\hat{D}$) vs RSE($\hat{D}$), (d) $1/\sqrt{\min\{\mathrm{E}(n), \mathrm{E}(r)\}}$ vs RSE($\hat{D}$).

Literature Cited

Clark, J. D. (2019). Comparing clustered sampling designs for spatially explicit estimation of population density. Population Ecology, 61, 93–101.

Efford, M. G. (2019). secrdesign: Sampling Design for Spatially Explicit Capture-Recapture. R package version 2.5.7. https://CRAN.R-project.org/package=secrdesign.

Kristensen, T. V., & Kovach, A. I. (2018). Spatially explicit abundance estimation of a rare habitat specialist: implications for SECR study design. Ecosphere, 9(5):e02217. doi: 10.1002/ecs2.2217